2020 IEEE/RSJ International Conference on Intelligent Robots and Systems (IROS)
October 25-29, 2020, Las Vegas, NV, USA (Virtual)

Wet Adhesion of Micro-patterned Interfaces for Stable Grasping of Deformable Objects

Pho Van Nguyen, Quan Khanh Luu, Yuzuru Takamura, and Van Anh Ho [1]

2020 IEEE/RSJ International Conference on Intelligent Robots and Systems (IROS) | 978-1-7281-6212-6/20/$31.00 ©2020 IEEE | DOI: 10.1109/IROS45743.2020.9341095

Abstract— **Stable grip of wet, deformable objects is a challenging task for robotic grasping and manipulation, especially for food products' handling. The wet, slippery interfaces between the object and robotic fingers may require larger gripping force, resulting in higher risk of damaging the grasped object. This research aims to evaluate the role of micro-patterned soft pad on enhancement of wet adhesion in grasping a food sample in wet environment. We showcased this scenario with a tofu block $19.6\times19.6\times15\,\mathrm{mm}^3$ that is soft, and deformable object, gripped by a soft robotic gripper with two fingers. Each fingertip's surface, which directly makes contact with the tofu, was deposited soft pads in two cases: normal pads (flat surface) and a micropatterned pads. The micropatterned pad comprises of 14400 square cells, each cell has four $85\,\mu$m edges, surrounded by a channel network with $44\,\mu$m in depth. We conducted estimation of grasped force generated by pads in two cases, then verified by actual setup in griping the tofu block. Both estimated and experimental results reveal that the micropatterned pad decreased necessary load acting on the tofu's surface 2.2 times lower than that of the normal one, while maintaining the stability of the grasped tofu. The showcase in this paper supported the potential of micro patterns on soft fingertip in grasping deformable objects in wet environments without complicated control strategy, promising wider applications for robot in service section or food industry.**

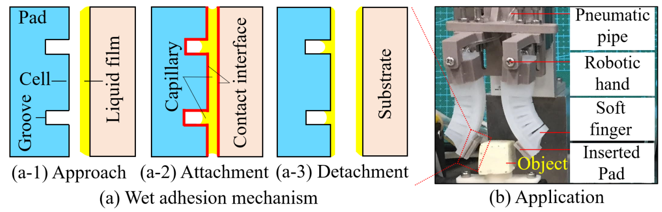

Fig. 1. A scenario of a soft fingered tip with a micropatterned pad in grasping a deformable object (tofu block): (a) Wet adhesion principle of the micropatterned pad in handling a wet substrate. In this case, the micropatterned pad approaches to the wet substrate (a-1), makes contact to the substrate (a-2), and detaches from the substrate (a-3). Such mechanism in (a) is applied to designing a soft robotic hand for autonomous grasping of a tofu block as a showcase of a deformable object in (b).

I. INTRODUCTION

Manipulating deformable objects may be benefited from applications of soft robots. Those objects in humans' daily life (for instance, food) or in medical field (such as tools, soft tissues) usually exist in wet conditions. That leads to difficulties for robotic devices in achieving stable grasp/manipulation of such objects without requiring high squeezing force (preload). One critical scenario is autonomous handling a tofu block (see Fig. 1(b)), by a robotic hand/gripper, including lifting off its container and subsequently positioning in an other places such as a lunch box. The tofu block is wet, deformable with extremely slippery surfaces. The grasped force in this case must be maintained at its minimum for avoiding large deformation on its surfaces, and the slippage. The utilization of adhesion could be solution to this task.

Some natural adhesion mechanisms introduced by Gorb [1] were applied to robotic applications. For instance, mimicking dry adhesive leg of a gecko for designing a patterned polymer can help a Stickybot to climb on walls [2]. Authors in [3] showed a design of a dielectric elastomer actuated gripper, which can generate electro-adhesion between the gripper and the objects. Nonetheless, these applications are appropriate with dry condition. Tree frogs [4] can firmly stick to their surrounding environments, thanks to the enhancement of wet adhesion generated from the microstructure on their toe pad [5]. This principle is appropriate to inspire the robotic fingers for gripping the deformable objects in wet environment w/o requiring high preload. Our study investigates the role of a micropattern, inspired by the wet adhesion of the tree frog's toe, on decreasing the deformation of the deformable object grasped by a soft robotic hand (Fig. 1(b)). The grasp forces were evaluated and compared in two cases: normal and micropatterned pads (n-pad and m-pad). In this scenario, the object had an available liquid film, while the pads were dry. Additionally, the mechanism of the wet adhesion of the contact interface between the pads and a substrate (object) followed three steps of grasping: approach, attach to, and detach from the substrate (Figs. 1(a-1)-(a-3)). Then, we carried out corresponding experiments to validate the estimation by grasping a tofu block as a showcase.

II. RELATED WORKS

A. Wet Adhesion with Pattern Design

Previous research showed that wet attachment mechanism inspired by the tree frog's pads can enhance the wet adhesion force. Chen *et al.* [6] designed a surgical gripper having pattern surfaces for increasing friction for grasping tissues. Authors in [7], [8] performed testings of wet friction force in study cases of the micropattern with changing hexagonal shape. Authors in [9]–[11] also presented the comparisons of the wet adhesion force between the micro-pillar surfaces. They showcased diverse experimental results, nonetheless, not many research proposed analytical models for systematic

This paper was supported by JSPS KAKENHI Grant Number 20J14910.
[1]Authors are with the School of Materials Science, Japan Advanced Institute of Science and Technology (JAIST), 1-1 Asahidai, Nomi, 923-1292 Japan. Email: pho.nguyen@jaist.ac.jp

investigation on reducing deformation of the objects with wet adhesion obtained from the m-pad-based grasp.

B. Previous Work

Our previous works constructed an analytical model, validated by experiments, to investigate the wet adhesion force for the flat contact interface between a m- and n-pad with a substrate [5], [12]. As a result, the adhesion force of the m-pad raised roughly 2-fold compared with that of the n-pad. Recently, the theoretical model in [5], [12] was developed to constitute an actual application in grasping a thin elastic shell such as a soft contact lens [13]. In fact, food or fruit posses soft, fragile feature with visco-elastic or rheology characteristics which require a thorough investigation.

C. Contributions

Our study made contributions as followed:

1) Proposed a theoretical model for investigating griping ability of a soft robotic hand with m-pad over a deformable object such as the block of tofu. This study is potential for extending to grasping deformable objects in wet conditions by m-pad fixed on the fingertips.
2) Proposed a design of a soft robotic hand which can grip and release the fresh tofu block and related pilot experiments for evaluation of the robotic hand's graspability on deformable objects in wet condition.

III. REVISIT THEORY OF VISCOELASTIC DEFORMATION AND WET ADHESION

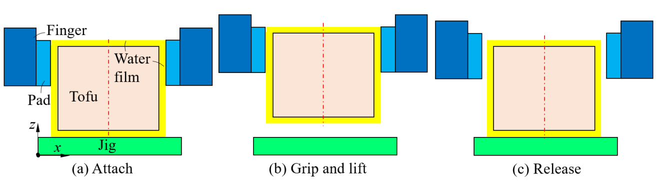

Fig. 2. Scheme of grasping a tofu by the soft robot. The fingers approaching (a), gripping and lifting away (b), and releasing the tofu on the jig (c).

A deformable object is grasped and released by a soft gripper (Fig. 2), and a fresh tofu is illustrated as a showcase. This section discussed through formulations that can explain the underlying physics of phenomena in gripping the tofu.

A. Deformation of the Deformable Object

The tofu contains primary ingredients from the soy protein and 90 %water [14], and was considered as a viscoelastic materials including: viscosity and elasticity upon deformation [15], [16]. In Fig. 3(a), the tofu having a cubic shape with edge length e_t is squeezed by the preload $P = pA_p$ generated from the pads to create the grasp force F_g. This generates the normal deformations Δe_t with the internal stress σ. Let us virtually divide the volume of the tofu into a system consisting of dashpot and spring elements, which are exerted

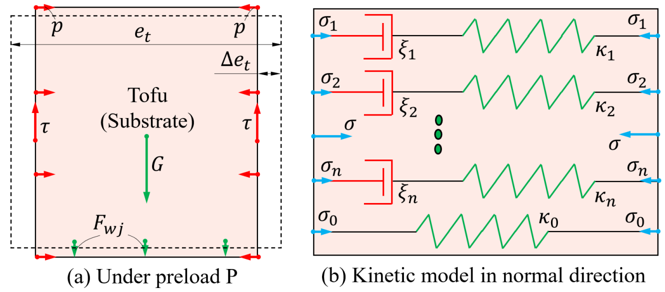

Fig. 3. Deformation model of the tofu in grasping (a) and (b) modelling the tofu by a spring element κ_0 and series of parallel viscoelastic elements comprising of a spring (κ_i) and a dashpot (ξ_i). τ is shear stress on the tofu surface.

by the normal stress σ_i in Fig. 3(b). According to [17], the relationship of stress-strain is given as followed:

$$\sigma = \sigma_0 + \sum_{i=1}^{n} \sigma_i = \kappa_0 \varepsilon_0 + \sum_{i=1}^{n} \frac{\kappa_i \xi_i \dot{\varepsilon}_i}{\kappa_i + \xi_i \dot{\varepsilon}_i}, \quad (1)$$

with $\varepsilon_i, \dot{\varepsilon}_i$ are respectively the strain and its deviation by time t of the element i. And the apparent modulus $\kappa(t)$ of the sample in relaxation state satisfies the followed expression:

$$\kappa(t) = \kappa_0 + \sum_{i=1}^{n} \kappa_i e^{-t\kappa_i/\xi_i}. \quad (2)$$

The Eqs. (1) and (2) show the scenarios of the tofu in cases: a small and a large (relaxation stress) deformations. As F_g does not generate a large deformation ($\varepsilon_i < 10\%$ [15]), we can neglect variation of the elastic modulus in Eq. (2).

B. Wet Adhesion in the Contact Interface

The water always existing both inside body and on the surfaces of the tofu, generates slippage during contacting with the pads. However, when the water is thin enough, it also enhances F_g thanks to the wet adhesion force F_w through formation of the capillary bridges in the contact interface (Fig. 5). Let us assume that the pads have parallel contact with the tofu's surfaces (Fig. 5(c)) with an interface gap h. According to [12], [18], F_w can be estimated as followed:

$$\mathbf{F}_w = \mathbf{F}_L + \mathbf{F}_{st} + \mathbf{F}_v, \quad (3)$$

where $\mathbf{F}_L, \mathbf{F}_{st}, \mathbf{F}_v$ are Laplace, surface tension and viscosity force vectors, respectively.

Investigation of F_w is performed by specifying the capillary's profile comprising of R_1 and R_2 (Fig. 5(c)). Hence, the Laplace pressure P_L equals ζ/R_1 with $1/R_2 \approx 0$ [12], [18]. Let r_w be the wet radius of the capillary, the Laplace force F_L, and the surface tension force F_{st} are respectively equal to $P_L \pi r_w^2$, and $2\zeta\pi r_w$. Also, we get the viscosity force F_v from the formulations $F_{v,n} = 1.5\pi\xi r_w^4 \dot{x}/h^3$ and $F_{v,t} = \xi \dot{z} \pi r_1^2/\lambda_2$ for normal and tangential directions, respectively.

IV. MECHANICS OF GRASPING WITH WET ADHESION

A. Design Robotic Hand

In Fig. 4(a), the soft robotic hand comprises of two symmetrical fingers constructed from a PneuNet structure,

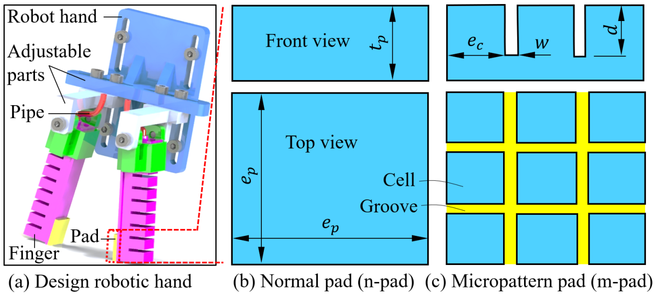

Fig. 4. Design of a soft robotic hand a) with two types of the fingertip pad: (b) n-pad (normal pad) and (c) m-pad (micropattern pad).

and fingertip pads were designed in two cases for evaluation: n- and m-pad (Fig. 4(b-c)). Such pads have a square shape with edge length e_p, thickness t_p and same materials. For the m-pad, it is patterned by n_c square cells having edge size e_c, interspaced by a network of the grooves having width and depth $w \times d$. This hand was fixed to a linear motorized stage functioned as a robotic arm. As pressurizing the fingers, the pads approach towards sides of the object for creation of F_g.

B. Modelling Grasping of a Wet Object

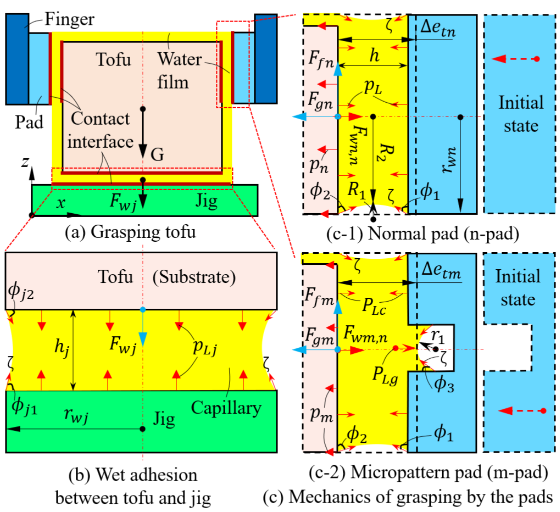

Fig. 5. Mechanics of grasping a tofu by the soft robotic fingers (a). (b) Contact model of the tofu's bottom with the jig. (c) Zoom-in illustration of contact interfaces in two cases: n-pad (c-1) and m-pad (c-2). p_n, p_m and $\Delta e_{tn}, \Delta e_{tm}$ are the preload pressure and normal deformation of the tofu. The dash lines and the dash-red arrows show the original states of the pads and the substrate, and the moving direction of the pads. $\phi_1, \phi_2, \phi_3, \phi_{j1}, \phi_{j2}$, ζ, ξ, h and r_w, r_{wj} are the contact angles, surface tension, viscosity coefficient, interface gap, and wet radii of the pad and jig, respectively.

For the m-pad (Fig. 5), upon contacting with the tofu, the water film on the tofu surface is sucked into the grooves as $w < h$. This phenomena can be explained through the relation of the Laplace pressures inside the groove $P_{Lg} \sim 2\zeta \cos\phi_3 / w$ and at the contact interface between cell and the substrate $P_{Lc} \sim \zeta(\cos\phi_1 + \cos\phi_2)/h$ [12].

In each of the corresponding contact interface, $\mathbf{F}_g$ generates the friction force $\mathbf{F}_f$, and the force $\mathbf{F}_w$ increases the stick ability with the pads. We also consider that the couple interfaces between the pad and the tofu's surfaces is completely parallel to z axis in the grasping scenario. In the equilibrium state, the tofu is lifted only if the tangential contact force $\mathbf{F}_{c,t}$ generated from the pad satisfies the followed conditions:

$$0.5(\mathbf{G} + \mathbf{F}_{wj}\hat{z}) \leq \mathbf{F}_{w,t} + \mathbf{F}_f = \mathbf{F}_{c,t}, \tag{4}$$

with $\hat{z}, F_{w,t}$ are unit vector of z-axis and tangential wet adhesion force. Here, the gravity $G = mg$ is considered constant, and the wet adhesion force with the jig $F_{wj} \approx \zeta(\cos\phi_{j1} + \cos\phi_{j2})\pi r_{wj}^2 / h_j + \zeta \sin\phi_{j1} 2\pi r_{wj}$. Thus, it is necessary to determinate other components in the right hand side of Eq. (4). This equation is utilized to compare the minimum preload pressure $\{p_n, p_m\}$ causing deformation on the tofu.

1) In Normal Direction (along $x-axis$): In Fig. (5), as there are no slip between the pad and the substrate, the capillary's shape has no significant change and the related velocity $\dot{x}, \dot{z}$ are neglected. According to [12], by synthesizing F_w the Eq. (3), the normal wet adhesion force in case the n-pad $F_{wn,n}$ is generally calculated as followed:

$$F_{wn,n} = e_p 4\zeta\left(e_p \vartheta + \sin\phi_1\right), \tag{5}$$

where $\vartheta = 0.25(cos\phi_1 + cos\phi_2)/h, \vartheta_1 = e_p^2/(e_c n_c) - e_c$. In the case the m-pad, the normal wet adhesion force $F_{wm,n}$ includes the Laplace, surface tension and Stefan force of the cells and the grooves [5]. Hence, the force $F_{wm,n}$ becomes:

$$F_{wm,n} = 4n_c e_c \zeta\left(\vartheta_1 \frac{\cos\phi_3}{2w} + e_c\vartheta + \frac{sin\phi_1}{\sqrt{n_c}} + \Delta n_c \cos\phi_3\right). \tag{6}$$

Note that $\psi_n = F_{wn,n}$ and $\psi_m = F_{wm,n}$ which are respectively in the left hand side of Eqs. (5) and (6), then F_g for the n-pad case F_{gn} and m-pad case F_{gm} become:

$$\begin{cases} F_{gn} = \pi r_w^2 p_n + \psi_n, \\ F_{gm} = \pi r_w^2 p_m + \psi_m \end{cases}. \tag{7}$$

Eq. (7) shows that F_{gn}, F_{gm} depend on $p_n, p_m, F_{wn,n}, F_{wm,n}$. The increment ratio of the grasp force in this scenario is:

$$r_g = \frac{F_{gm}}{F_{gn}} = 1 + \frac{2\zeta\cos\phi\left[(2 + 2\Delta n_c - 1/\lambda_2)/e_c + 1/h\right]}{p(1+1/\lambda_1)^2 + 2\zeta\cos\phi(1+1/\lambda_1)^2/h}, \tag{8}$$

where $\lambda_1 = e_c/w, \lambda_2 = h/w, \Delta n_c = 1 - n_c^{-0.5}$, and we assume that $\phi = \phi_1 = \phi_2 = \phi_3$. Because the design of the m-pad satisfied $w < h$, the increment ratio r_g in Eq. (8) is always larger than one in case $p_m = p_n = p$. In other words, in case grasping the tofu by the m-pad, $F_{wm,n}$ significantly enhances F_{gm} than that of grasping by the n-pad. This plays an important role in the following sections as the normal force is a principal component in grasping.

2) In Tangential Direction (along $z-axis$): F_{gn}, F_{gm} in Eq. (7) generates F_f and the tangential wet adhesion force $F_{w,t}$. This study only focuses on investigating the tangential contact force $F_{c,t}$ in incipient slip ($\dot{z} = 0, F_{w,t} \sim 0$). Also we have $F_f = \eta F_{gn}$ [19] with η is the friction coefficient. According to [12], projecting Eq. (3) in z axis yields $F_{c,t}$ in case the n-pad as followed:

$$F_{cn,t} = \eta_n(p e_p^2 + \psi_n). \tag{9}$$

And the tangential contact force in case the m-pad becomes:

$$F_{cm,t} = \eta_m(pe_p^2 + \psi_m). \tag{10}$$

From the Eqs. (9) and (10), the increment ratio of the tangential contact force $r_t = F_{cm,t}/F_{cn,t}$ is calculated as followed:

$$r_t = \frac{\eta_m}{\eta_n}\left[1 + \frac{2\zeta\cos\phi\,[(2+2\Delta n_c - 1/\lambda_2)/e_c + 1/h]}{\lambda_{21}(p + 2\zeta\cos\phi/h)}\right], \tag{11}$$

with $\lambda_{21} = (1+w/e_c)^2, \lambda_{22} = w(2+w/e_c)/e_c$. It is similar to the conclusion in Eq. (8), r_t in Eq. (11) is also larger than the ratio of the friction coefficients of m- and n-pad η_m/η_n. On the other hands, comparing the value of r_t with 1 depends on the ratio $\{\eta_m/\eta_n\}$. When $\eta_m = \eta_n$, r_t becomes r_g. That reveals the micropattern can create a stronger enhancement of the wet adhesion in tangential contact force than that of the normal surface. Replacing Eqs. (9) and (10) into Eq. (4) yields the preload pressure p_n of the n-pad as followed:

$$p_n \geq 0.5(G + F_{wj})e_p^{-2}/\eta_n - \psi_n/e_p^2, \tag{12}$$

and that of the m-pad case is:

$$p_m \geq 0.5(G + F_{wj})e_p^{-2}/\eta_m - \psi_m/e_p^2. \tag{13}$$

Dividing the right hand side of Eq. (13) into that of Eq. (12) yields the reduction ratio of the minimum preload pressure $r_p = min\{p_m\}/min\{p_n\}$ as followed:

$$r_p = \frac{\eta_n}{\eta_m}\left\{1 - \frac{1 + [\lambda_{22}(\lambda_1 - 1) + 2\Delta n_c\lambda_2/\lambda_1]/\lambda_{21}}{0.5(G+F_{wj})/\psi_n - 1}\right\}. \tag{14}$$

The ratio r_p in Eq. (14) is smaller than 1 that is equivalent to $min\{p_m\} < min\{p_n\}$ because we consider $\eta_m = \eta_n$ and $\lambda_1 > 1$. In addition, this ratio gradually decreases as $\eta_m > \eta_n$. The deformation of the tofu, in this study, is so small for concerning the relaxation stress. Thus, the apparent elastic modulus $\kappa(t)$ in Eq. (2) can be neglected. For simplicity, let us assume that the preload pressure is similar at every point on the contact interfaces, which leads to the same strain ε_i in Eq. (1) at all contact points. Combining Eqs. (1) and (14) yields the reduction ratio $r_s = \varepsilon_{im}/\varepsilon_{in}$ for the strains between the m-pad case and the n-pad case as shown in Eq. (15):

$$r_s = 1 - \frac{p_n e_p^2(1-r_p) + \sum_{i=1}^n \xi_i\kappa_i^2(\dot{\varepsilon}_{im} - \dot{\varepsilon}_{in})/(\chi_{in}\chi_{im})}{p_n e_p^2 - \sum_{i=1}^n \kappa_i\xi_i\dot{\varepsilon}_{in}/\chi_{in}}, \tag{15}$$

where $\chi_{in} = \kappa_i + \xi_i\dot{\varepsilon}_{in}, \chi_{im} = \kappa_i + \xi_i\dot{\varepsilon}_{im}$.

Consequently, gripping the tofu with the m-pad requires a smaller value of P exerting on the tofu's surfaces. In addition, Eq. (15) reveals that grasping in case the m-pad has less damage for the substrate.

V. EXPERIMENTAL RESULTS

A. Fabrication

A micro-patterned mold (m-mold) was fabricated by a lithography method, with size of $12\times12\,\text{mm}^2$. The fabrication process is summarized as followed:

1. The silicon wafer was cleaned to remove the organic residues from the surface.

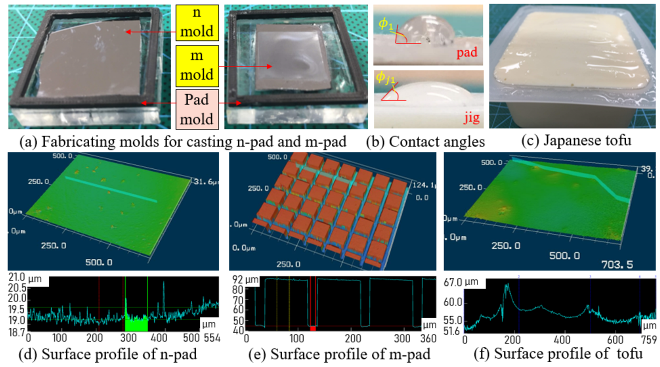

Fig. 6. Fabrication processing of the pad and preparing sample. The n- and m-pad molds (a) were fabricated by fixing the silicon substrates on the glasses. (b) Measuring the contact angles of the pad and the jig. (c) A Japanse tofu as a sample for experiments. (d), (e) and (f) the surface profiles of the n-pad, m-pad and the tofu. Error of w is roughly 15 %.

2. Maskless lithography device (Heidelberg MLA150) was used to create square pattern with line-width of 15 μm on Su-8 3050 photoresist.
3. The resit was developed in Su-8 developer for generating the micro-patterned with the depth of 44 μm.
4. The silicon substrate with micro-pattern was washed by water and dried with N_2 before testing in the laser scan microscope (Keyence VK-9710, Japan).

The obtained m-mold was then fixed in a larger mold for casting silicon rubber (Ecoflex 00-50, SmoothOn, USA) to create the m-pad with thickness of 1 mm (Fig. 6(a)). Cells on the m-pad have the length of 85 μm$\times$85 μm, separated by the grooves with $15\,\mu m \times 44\,\mu m$ in width and depth. The surface of m-pad, n-pad and the substrate were observed in laser scan microscope (VK-9710, Keyence, Japan) in Figs. 6(d-f). Generally, the cell's surfaces of the m-pad is more smooth than that of the n-pad and the tofu. The high roughness areas is very small on the surfaces of the n-pad (maximum $\sim 1\,\mu m$) and the tofu (maximum $\sim 12\,\mu m$). The fingers following the Pneunet structure and the cover layer were made from DragonSkin 00-10 and DragonSkin 00-20. The other parts of the robotic hand were printed by 3D Zotrax M200 with using ABS plastics. Also we cut a Japanese tofu with it dimensions: $19.6\times19.6\times15\,\text{mm}^3$ as a sample to carrying out for the test (Fig. 6(c)). The surface having edge's length $19.6\times19.6\,\text{mm}^2$ was implanted by black markers (ABS plastic) for tracking the deformation of the sample (see Fig. 11 for details).

B. Experimental setup

The experiment set-up is shown in Fig. 7. Here, the fabricated m- or n-pads were fixed on the tips of a pair of pneumatic fingers. The robotic hand was attached to a motorized linear stage which can provide precise movement along vertical z axis. The two soft fingers were connected through plastic pipes to a syringe pump whose plunger is fixed onto a horizontal linear stage (x-slide). Both of the linear stages were driven by a stepping motor controller (Suruga Seiki D212). The formation of the pneumatic fingers' grasping pose, as well as wide range of initial loads

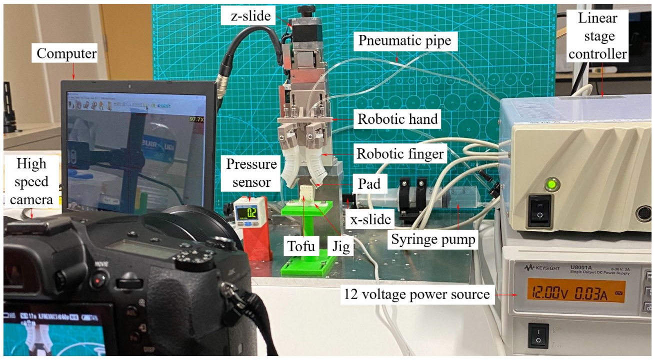

Fig. 7. Scheme of experimental set-up for measuring the preload.

exerting on the piece of tofu at the fingertips, were regulated by varying air pressure, using the syringe pump. The acting pressure was measured by a pressure sensor (SMC ISE30A). Moreover, in order to evaluate the deformation of the piece of tofu under a designated acting pressure, a high-speed camera (Sony DSC-RX10M4) with 24 frames per second is used to capture black markers attached onto the surface of the tofu. During the evaluation process, the wet adhering

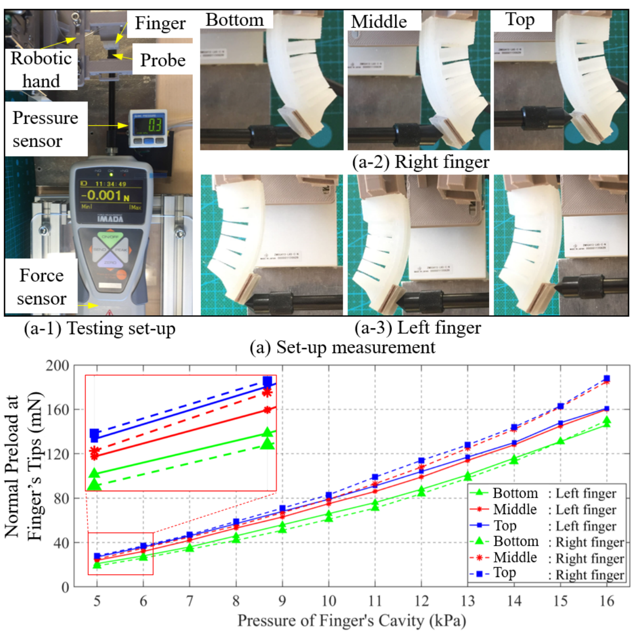

Fig. 8. Measuring the preload by calibrating the pressure inside the Pneunet structure of the robotic fingers. The measurement set-up in a) including a pressure sensor and a force sensor a-1). Also the tests were performed at three points on two fingers a-2) and a-3). b) Results of the force calibration.

capabilities of the n-pad and m-pad were examined by two main phases: grasping pressure and releasing pressure. In the first phase, a minimum pressure (*i.e.*, grasping pressure) was determined, which was just sufficient enough to lift the tofu block out of the jig and then firmly held it without being slipped, while the hand was kept at a certain height. In order to obtain this *grasping pressure* value, at first, the robotic hand moved down to the piece of tofu. Next, the soft fingers were actuated so that the air pressure (*i.e.*, initial load) exerting on the tofu was gradually increased. In the second phase, once the robotic hand moved the tofu to a certain height, the exerting pressure was being steadily reduced until the tofu started sliding on the surfaces of the soft pads. The pressure at which the slippage occurred was defined as *releasing pressure*. Then, the preload P exerting on the surfaces of the pads were obtained by calibration the input pressure inside the chamber of each fingers as shown in Fig. 8(a). The calibration tests returned results for the preload at 3 positions: top, middle and bottom of the pad as illustrated in Fig. 8(a-2)(a-3). The value of preload was almost similar for two fingers as the low pressure ($P < 10\,kPa$); whereas, as ($P >> 10\,kPa$), the preload of right finger is 10% higher than that of the left finger (Fig. 8(b)). This error came from the accumulated error at large deformation of the fingers, which generated the different slope angle of the pad along z-direction. The difference in fabrication of two fingers may also be a reason.

C. Evaluation results

TABLE I
PARAMETERS OF GRASPING MODEL

m (g)	ξ (N/m)	ϕ (rad)	ϕ_j (rad)	h,h_j (μm)	η_n, η_m
5.537	0.073	1.41	0.77	25,30	0.35

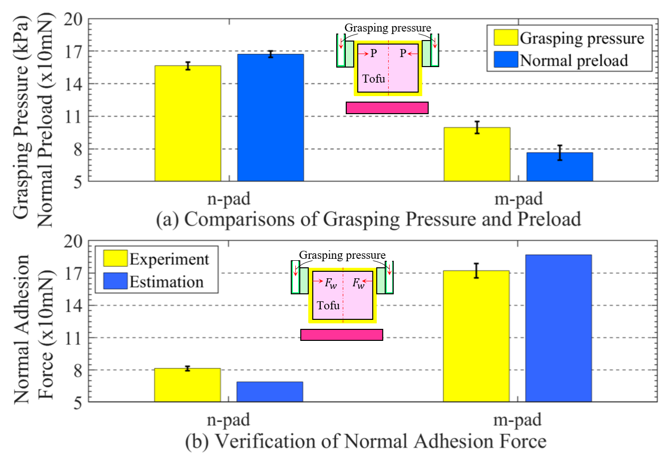

Fig. 9. Comparison of the force value from the pads exerting on the tofu between two cases: n-pad and m-pad. (a) The grasping pressure and its corresponding normal preload P was obtained from the mean value of the left and right fingers at middle position (Fig. 8(b)). (b) Verification of the normal adhesion force F_w derived from Eq. (4) with replacing the experimental value of P (equals to F_{gn}, F_{gm}) in (a). The force F_{wn} of the n- and m-pad were, in turn, calculated in Eqs. (5) and (6). The condition for this calculation was measured in Fig. 6(b) and referred in table I, πr_{wj}^2=45.396 mm^2, $2\pi r_{wj}$=90.79 mm.

1) Grasping pressure: The grasping pressure and the resulted normal preload by which the designed robotic hand could stably lift the piece of tofu were experimentally observed in 5 trials for each type of the soft pads (m-pad or n-pad). The obtained data is statistically processed and shown in the Fig. 9(a). It reveals that the n-pad needs a higher grasping pressure to firmly lift the tofu, at approximately 15.7 kPa, thus leading to the normal preload of 168 mN. Whereas, with the m-pad, the grasping pressure of the robotic hand required for safely handling the tofu is smaller than that of the n-pad, with the mean value of 10 kPa and its corresponding normal preload is at about 75 mN. From the initial conditions in Fig. 9, we have G= 0.054 N and F_{wj}= 0.12 N. By replacing the obtained results of the preload in the Fig. 9(a) into Eqs. (4), (9) and (10) we had the experimental data of the adhesion forces with $\bar{F}_{wn,n}$= 0.0812 N, $\bar{F}_{wm,n}$= 0.173 N. The testing values of the normal adhesion force were utilized to validate the estimation in Eqs. (5) and (6) which returned wet adhesion forces of n- and m-pad are $F_{wn,n}$= 0.0692 N and $F_{wm,n}$= 0.187 N, respectively (Fig. 9(b)). The comparison showed a good agreement between the analytical model and the evaluation experiment, when the errors of the normal adhesion force are -14.8 % and 8.09 % for the n- and m-pad, respectively. This reveals that the m-pad needs lower applied preload into the tofu comparing with that of the n-pad ($\bar{r_p}$= 7.57 N/0.1667 N=0.454<1, respectively). In other words, the ratios $\{r_g, r_t, r_p\}$ in Eqs. (8), (11) and (14) are both appropriate with the actual tests.

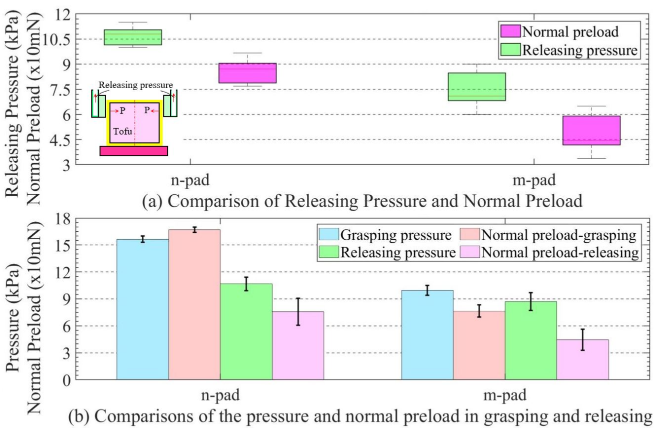

Fig. 10. Releasing pressure and its corresponding normal preload P of the n- and m-pad (a), and comparing with that of in grasping phase (b). P was obtained in the same way as shown in Fig. 9.

2) Releasing pressure: The examining results of releasing pressure was determined at the moment the tofu started sliding relatively to the surface of the soft pads, judged through high-speed camera. Fig. 10(a) shows the releasing pressure repeated 5 trials for two cases of pads: n- and m-pad. For the n-pad, the recorded releasing pressure slightly fluctuates around 10.7 kPa, then its resulting normal preload is at 94 mN, which is lower than the grasping pressure and the preload by 5 kPa and 74 mN, respectively (Fig. 10(b)). Regarding the m-pad-type hand, the releasing pressure varies greatly, ranging from 6.5 to 8 kPa with the mean value of roughly 7 kPa, and thus differentiating from the grasping one by more or less 3 kPa. Also, the corresponding normal preload of 41 mN observed in the releasing state is lower than that of the grasping state, by 34 mN (Fig. 10(b)).

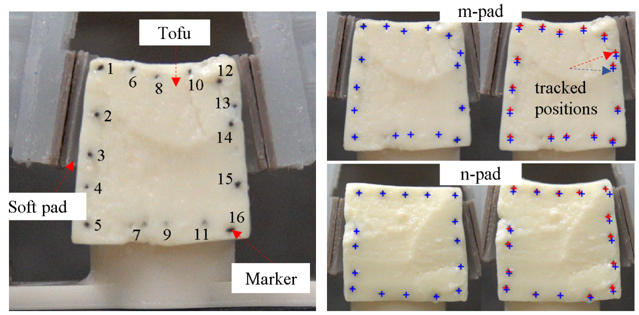

(a) Set-up for tofu-deformation evaluation (b) Pre-grasp state (c) Deformed state

Fig. 11. The figure (a) shows the high-speed camera view for marker tracking which is used for determination of tofu deformation, (b) illustrates the tracked markers' positions in the original state of the tofu and (c) demonstrates the changes in markers' positions when the tofu is subjected to an acting force, and then gets to the deformed state.

3) Tofu Deformation: In this section, we report evaluation on how the piece of tofu was deformed under a preload (*i.e.*, grasping pressure), exerted by the robotic hand equipped with the normal n- and m-pad. Black markers (16 in total) were arranged on the front surface of the tofu, with ordinal numbers as shown in Fig. 11(a), then their relative positions could be tracked and measured using the Image Processing tool in MATLAB software. The deviation of markers' positions (marked as red 'plus' sign) on the tofu under the acting force (*i.e.*, deformed state in Fig. 11(c)) from that of the original state (marked as blue 'plus' sign in Fig. 11(b)) was measured to assess the change in the tofu shape in terms of two-dimensional deformation. The deformation was observed in two cases: the tofu was gripped by the m- and n-pad under a grasping pressure of 10kPa and 15.7kPa, respectively. Because the markers are not arranged neatly onto the surface of the tofu, whose shape is badly defined in the pre-grasp state as well, it is hard to observe and evaluate the changes in the tofu shape under the grasping forces. In order to recognize the deformed tofu shape, therefore, we modelled the piece of tofu by translating the tracked markers' position to new calculated ones such that the original modelled tofu would transform to a square shape (c_0).

With the same translation for tracked markers in the deformed state, the model shows that in the both cases under the preload, the upper and bottom sides of the tofu are substantially deformed so that their contours would fit well as parabolic curves (c_1) (Fig. 12(a-1)). However, experiencing a large force - in the case of n-pad, the tofu is by more deformed at the corners and edges, which is modelled into the contour of (c_2) (Fig. 12(a-2)). Moreover, the deformation is analytically evaluated by measuring maximum strains with respect to x-axis and z-axis, which are calculated by the changes in length (ΔL=L-L_0) of the specific axis over the initial one (L_0) (Fig. 12(a-2)). According to the figure of two-dimensional deviation presented in Fig. 12(b) and the original lengths of the tofu (L_{0x}=19.6 mm, L_{0z}=19.6 mm), the maximum changes in length in terms of the case 1 (m-pad) are by -0.22 mm (ΔL_x=Δx_{12}-Δx_5, the minus sign

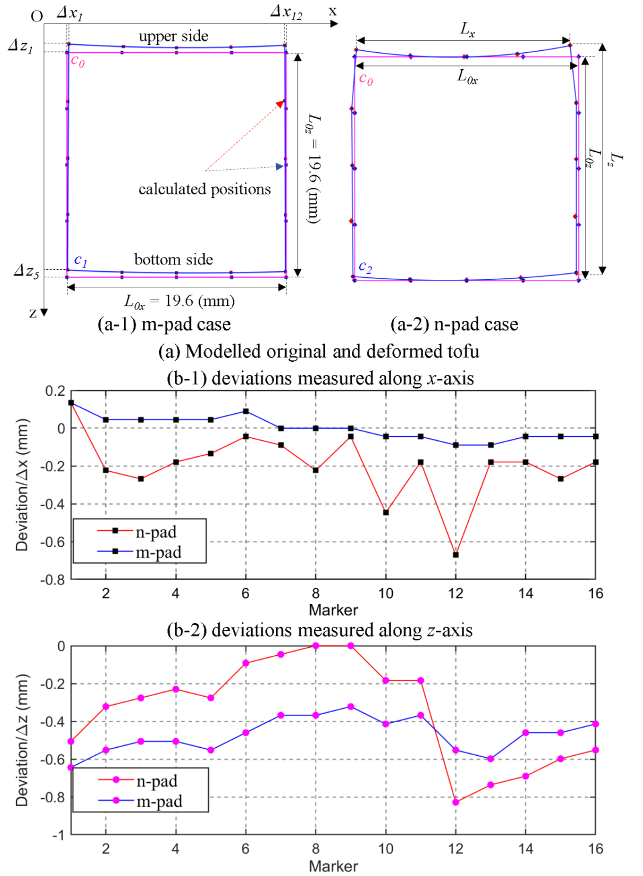

(b) 2-dimensional deviations of 16 markers

Fig. 12. The figure (a) illustrates the model of the tofu seen from the front side after translating the tracked markers' positions to the calculated ones. (a-1) and (a-2) are the tofu models derived from the experiment with case 1) m-pad and case 2) n-pad, in which (c_0), (c_1) and (c_2) are original and deformed tofu contours in case 1 and case 2, respectively. (b) the graph shows the deviation of the original markers from the deformed ones with respect to the 16 markers, which are measured in two dimensions, (b-1) x-axis (Δx_1 to Δx_{16}) and (b-2) z-axis (Δz_1 to Δz_{16}).

means the length reduced over the initial length) and 0.09 mm (ΔL_z=Δz_5-Δz_1) along the x and z direction, respectively, and consequently the strains in turn are 1.14 % and 0.47 % (Fig. 13). The deformation in the case 2 (n-pad) is considerably larger in comparison to the first case, that is, the maximum strains calculated in that case are 4.11 % along the x direction and 1.41 % along the z one (Fig. 13). Also, the changes in length are nearly four times as large in the x direction as that of the m-pad gripping case, at -0.81 mm (ΔL_x=Δx_{12}-Δx_5) and twice in the z direction, at 0.28 mm (ΔL_z=Δz_{16}-Δz_{12}). These obtained results repeatedly reveal that the m-pad exerted a smaller preload P which caused the major deformation of the tofu, comparing with that of the n-pad. In other words, testing the strain of the tofu also contracted with the reduction ratios $\{r_p, r_s\}$ in Eqs. (14) and (15).

VI. Conclusion

Through enhancing the wet adhesion in grasping the tofu, the micropattern performed its role on decreasing the preload

Fig. 13. The strain of tofu exerted by the m-pad robotic hand along the x and z axes, compared with that induced by the n-pad one.

and deformation of the defor mable objects by estimation and testing. The obtained results contributes a foundation for the study of mechanics in gripping deformable objects in wet conditions. In the future, more morphology of the micropattern would be investigated with other similar objects in wet and moisturized environment.

References

[1] S. N.Gorb, "Biological attachment devices: exploring nature's diversity for biomimetics", *Phil. Trans. R. Soc. A*, Vol. 336, 2008.

[2] S. Kim *et al.*, "Whole body adhesion: hierarchical, directional and distributed control of adhesive forces for a climbing robot", *IEEE International Conference on Robotics and Automation (ICRA)*, pp. 1268-1273, 2007.

[3] J. Shintake *et al.*, "Versatile soft grippers with intrinsic electro adhesion based on polymer actuators", *Adv. Mater.*, Vol. 28, 2016.

[4] W. Federle and J. Smith, "Wet but not slippery: boundary friction in tree frog adhesive toe pads", *J. R. Soc. Interface*, Vol. 3, 2006.

[5] P. V. Nguyen, N. V. Huynh, T. T. Phan, and V. A. Ho, "Soft grasping with wet adhesion: preliminary evaluation", *2018 IEEE International Conference on Soft Robotics (RoboSoft)*, pp. 418-423, 2018.

[6] H. Chen, L. Zhang, and Z. Han,"Bioinspired surface for surgical graspers based on the strong wet friction of tree frog toe pads", *ACS Appl. Mater. Interfaces*, Vol. 7, 2015.

[7] M. Varenberg and S. N. Gorb,"Hexagonal Surface Micropattern for Dry and Wet Friction", *Adv. Mater.*, Vol. 21, 2009.

[8] J. Iturri *et al.*," Torrent frog-inspired adhesives: Attachment to flooded surfaces", *Adv. Funct. Mater.*, Vol. 25, pp. 1499-1505, 2015.

[9] F. Meng *et al.*, "Tree frog adhesion biomimetics: Opportunities for the development of new, smart adhesives that adhere under wet conditions", *Phil. Trans. R. Soc. A*, Vol. 377, No. 2150, 2019.

[10] J. Li *et al.*, "Mechanisms Underlying the Biological Wet Adhesion: Coupled Effects of Interstitial Liquid and Contact Geometry", *J Bionic Eng*, Vol. 17, pp. 448–456, 2020.

[11] M.Li *et al.*, "Effect of wetting case and softness on adhesion of bioinspired micropatterned surfaces", *J Mech Behav Biomed*, Vol. 78, pp. 266-272, 2018.

[12] P. V. Nguyen and V. A. Ho, "Mechanics of wet adhesion in interaction with patterned morphology", *Bioinspir. Biomim.*, Vol. 14, 2018.

[13] P. V. Nguyen and V. A. Ho, "Grasping Interface With Wet Adhesion and Patterned Morphology: Case of Thin Shell", *IEEE Robotics and Automation Letters*, Vol. 4, No. 2, pp. 792-799, 2019.

[14] K.A. Khatib *et al*, "Physicochemical Characteristics of Tofu Formulated from Selected Soybean Varieties", *J. Food Qual.*, Vol. 25, 2002.

[15] Y. Cheng, N. Shimizu, and T. Kimura, "Texture Evaluation of Tofu (Soybean Curd) by Viscoelastic Tests", *Japanese Society of Agricultural Machinery*, Vol. 64, Issue 6, pp. 137-144, 2002.

[16] Y. Cheng, N. Shimizu, and T. Kimura, "The viscoelastic properties of soybean curd (tofu) as affected by soymilk concentration and type of coagulant", *Int J Food Sci Technol*, Vol. 40, pp. 385–390, 2005.

[17] G. L. Danton, *Engineering Viscoelasticity*, Springer US, 2014.

[18] H.-J. Butt, M. Kappl, "Normal capillary forces", *Advances in Colloid and Interface Science*, Vol. 146, pp.48-60, 2009.

[19] J. Gao *et al.*, "Frictional forces and amontons' law: the molecular to the macroscopic scale", *J. Phys. Chem. B*, Vol. 108, 2004.